

Modeling of Dendritic and Eutectic Microstructures in Solidification of Aluminum Alloys

M.F. Zhu¹, C.P. Hong²

¹ Department of Materials Science and Engineering, Southeast University, Nanjing 210096, China.

² Center for Computer-Aided Materials Processing (CAMP), Department of Metallurgical Engineering, Yonsei University, Shinchon-dong 134, Seodaemun-ku, Seoul, 120-749 Korea.

Keywords: microstructure simulation, modified cellular automaton, aluminum alloys, dendritic structure, eutectic structure

Abstract

A modified cellular automaton (MCA) model has been developed in order to predict the evolution of dendritic and eutectic microstructures in solidification of alloys. The MCA model accounts for the aspects including the heterogeneous nucleation of a new phase, the growth of primary dendrites and two eutectic solid phases from a single liquid phase, as well as the coupling between the phase transformation and solute redistribution. The present model was applied to predict the primary dendritic growth and eutectic structure formation during practical casting solidification of Al alloys. The simulated results were compared with those obtained experimentally.

1. Introduction

In the most widely used cast Al alloys, the principal microstructure features are the primary dendrites with interdendritic eutectics. These features can persist through subsequent processes and significantly affect the properties of the finished components. In order to predict and achieve desired microstructures and hence, obtain high quality castings, it is of primary importance to understand the mechanisms of microstructure formation. However, solidification is a complicated process controlled by the interplay of thermal, solute, capillary, and kinetic length or time scales. In order to better understand the underlying physics in this process, a complete time-dependent description of microstructure evolution become crucial. For this purpose, there is a considerable potential for applying numerical simulations to provide satisfactory information on the interactions between transport phenomena and phase transition during solidification. Indeed, with the development of powerful computers and advanced numerical technique, numerical modeling has made significant progress and is playing an increasing role in studies of the microstructural evolution during solidification [1]. Particularly, modified cellular automaton (MCA) models, which are developed based on previously classical CA models, have recently emerged as a viable computational tool for the prediction of dendritic or non-dendritic microstructure formation under various casting conditions [2-8]. A MCA model developed by the authors has also been extended into multi-phase systems to model the microstructure formation in regular and irregular eutectic, and peritectic alloys [9-12].

In this paper, MCA model is applied to model the formation of dendritic and eutectic microstructures during solidification of Al alloys. The simulation results compared with those obtained experimentally are presented.

2. Model Description

The present MCA model retains the probabilistic aspects of classical CA models, such as the heterogeneous nucleation, the preferential growth orientations of nuclei and the growth kinetics of a dendrite tip. However, different from classical CA models in which only the temperature field is considered, the MCA model also accounts for the curvature and the solute redistribution during solidification. The calculation domain is divided into uniform square arrangement of cells for the two dimensions (2-D) and uniform cubic cells for the three dimensions (3-D). Each cell is characterized by different variables (such as temperature, concentration, crystallographic orientation and solid fraction) and states, i.e., liquid or solid (α or β phases).

The continuous nucleation model [13] is adopted for describing the heterogeneous nucleation of primary dendritic and eutectic phases. The preferential growth orientations are in the ranges of θ ($0, \pi/2$) for non-faceted crystals, and φ ($0, \pi$) for faceted crystals for the 2-D simulation. In case of 3-D dendritic growth, the preferential growth orientations are characterized by three Euler angles, ϕ ($-\pi, \pi$), θ ($0, \pi/2$) and φ ($-\pi/4, \pi/4$), respectively.

Once a cell has nucleated or solidified, it will grow with a preferential direction corresponding to its crystallographic orientation. The growth velocity of an interface cell is dependent on the local undercooling. The local undercooling at time t_n , $\Delta T(t_n)$, is considered to be the sum of three contributions of solutal, thermal and curvature and is given by

$$\Delta T(t_n) = T_0 - T(t_n) + m \cdot (C(t_n) - C_0) - \Gamma \bar{K}(t_n) \quad (1)$$

where T_0 and C_0 are the equilibrium liquidus temperature and the initial composition. With respect to eutectic growth, T_0 and C_0 are the eutectic temperature and the eutectic composition. Γ is the Gibbs-Thomson coefficient, $\bar{K}(t_n)$, $C(t_n)$ and $T(t_n)$ are the mean curvature, the concentration and the temperature of an interface cell at time t_n , respectively. The calculation of interface mean curvature can be found in the literature [2,7].

Different algorithms for the growth of non-faceted and faceted crystals are employed. The growth length of an interface cell at time t_n , $l(t_n)$, is calculated as follows:

$$\text{Non-faceted crystal} \quad l(t_n) = (\cos \theta + |\sin \theta|)^{-1} \left(\sum_{n=1}^N \{v[\Delta T(t_n)] \times \Delta t_n\} \right) \quad (2)$$

$$\text{Faceted crystal:} \quad l(t_n) = \cos \theta \sum_{n=1}^N \{v[\Delta T(t_n)] \times \Delta t_n\} \quad (3)$$

where Δt_n is the time step, θ is the angle of the preferential growth direction of a solid cell with respect to the linking line between this solid cell and its liquid neighbor cell, and N indicates the iteration number. $v[\Delta T(t_n)]$ is the growth rate. In case of eutectic simulation, if

an interface liquid cell is neighbored by both α and β phase cells, the local undercoolings and the growth lengths with respect to the growth of α and β phases are calculated and compared simultaneously. The competitive eutectic growth is thus directly embedded in the MCA growth algorithm. The details of the algorithms for the growth of 2-D and 3-D dendrites, and 2-D eutectics can be found elsewhere [3, 5, 10].

It is assumed that the local equilibrium condition is maintained at solid/liquid interface and the solute field is mainly controlled by diffusion. For eutectic solidification, the solidified α phase cell rejects solute to its neighboring liquid cells. Conversely, the solidified β phase cell absorbs solute from its neighboring liquid cells. The governing equation for solute redistribution is given by

$$\frac{\partial C}{\partial t} = D\nabla^2 C + C(1 - k_\alpha) \frac{\partial f_{s,\alpha}}{\partial t} + (C - C_{\beta 0}) \frac{\partial f_{s,\beta}}{\partial t} \quad (4)$$

where D is the solute diffusion coefficient, k_α and k_β are the partition coefficients, $C_{\alpha 0}$ and $C_{\beta 0}$ are the solubility limits, and $f_{s,\alpha}$ and $f_{s,\beta}$ are the solid fractions of phases α and β , respectively. The second and third terms on the right hand side of Eq. (4) indicate the solute gain and loss resulting from an increase of solid fractions at the solid/liquid interface. Eq. (4) was numerically solved using an explicit finite difference scheme.

3. Results and Discussion

Figure 1 indicates the simulated and experimental macro- and micro-structures of Al-Cu alloys unidirectionally solidified with a pouring temperature of 1013K using the 2-D MCA model. The figures on the left column indicate the case of the Al-2.5mass%Cu and the right for the case of the Al-4.5mass%Cu. Figure 1 (a) and (c), the grain structures simulated by a classical CA model, are in good agreement with (e) and (g) obtained experimentally. For this simulation, the domain was divided into 1000×2000 cells with a cell size of $30 \mu\text{m}$. Figure 1 (b) and (d), the dendritic structures simulated by the MCA model, are also in good agreement with (f) and (h) obtained experimentally. For this simulation, the domain was consisted of 400×400 cells with a cell size of $3 \mu\text{m}$. Figure 3 exhibits that under an identical solidification condition, with the increase of solute content, the dendritic morphology is transformed from columnar to equiaxed. According to the theories of dendritic nucleation and growth kinetics [14,15], the bulk nucleation density increases, whereas the growth velocity of a dendrite tip decreases with an increase of solute content. Accordingly, the occurrence of heterogeneous nucleation in the bulk liquid will be favored, and hence lead to an equiaxed dendritic morphology in the Al-4.5mass%Cu alloy. It is noted that the MCA model is able to predict both columnar and equiaxed dendritic morphologies in castings.

The dendritic microstructures of gas-atomized Al-10 mass%Cu alloy droplets under the non-uniform temperature field condition have also been predicted by the 3-D MCA model. The calculation domain consists of 491,864 uniform cubic cells and the cell size is $1 \mu\text{m}$. The atmospheric temperature is considered to be 298K. The heat transfer coefficient at the droplet/air interface and the superheat of a droplet are chosen to be $5000 \text{W/m}^2\text{K}$ and 30K, respectively. Figure 2 indicates the simulated and experimental microstructures with various droplet sizes of (a) $40 \mu\text{m}$, (b) $100 \mu\text{m}$ and (c) $200 \mu\text{m}$, which are shown in 2-D section. Figure 2 (d) shows the three-dimensional outlook of dendritic morphology of a droplet with a diameter of $100 \mu\text{m}$. It can be noted that as the 2-D MCA model, the 3-D MCA

model can predict not only the solidification grain structures, but also the dendritic morphology inside grains.

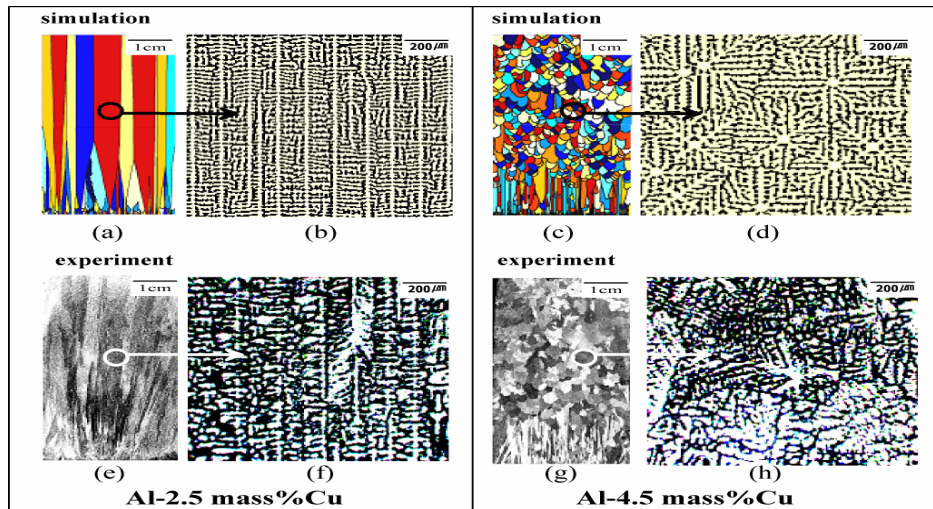


Figure 1: Simulated and experimental results in directional casting of Al-Cu alloys with a pouring temperature of 1013 K: (a), (b), (c) and (d) indicate the simulated results; (e), (f), (g) and (h) indicate the experimental results. (a) and (c) indicate the macrostructures simulated by a classical CA model, and (b) and (d) indicate the microstructures simulated by the 2-D MCA model.

The 2-D multi-phase MCA model was applied to predict the microstructures of eutectic and hypoeutectic Al-Si alloys. The calculation domain consists of 460×600 cells with a cell size of $3 \mu\text{m}$. In case of an Al-12.6mass%Si eutectic alloy, 60 eutectic nuclei having random growth orientations were randomly distributed at the bottom of the domain. In case of an Al-8mass%Si hypoeutectic alloy, 6 seeds of α -phase were additionally assigned according to the primary dendritic arm spacing observed in the experimental result. Figure 3 indicates the simulated and experimental [16] microstructures of directionally solidified Al-Si alloys with a constant thermal gradient of $G=15\text{K/mm}$: (a) Al-12.6mass%Si eutectic and (b) Al-8mass%Si hypoeutectic. The eutectic growth beginning from the bottom was interrupted by water quenching in order to observe the eutectic/liquid interface morphology. It can be noted from Figure 3 (a) that the faceted eutectic silicon flakes grow simultaneously with the non-faceted α matrix, having a wide range of local spacing and orientations with respect to the overall growth direction. In the quenched region there are some fine α dendrites which are present because the eutectic point is displaced to higher Si contents at rapid cooling. It is well accepted that rapid cooling rates skew the coupled growth regime, depressing the freezing point, and shifting the eutectic point to higher Si levels [17]. On the other hand, Figure 3 (b) indicates that the primary α dendrite and interdendritic eutectic coexist in this hypoeutectic Al-Si alloy. Besides, compared with Figure 3 (a), much thicker dendrites exist in the quenched region of Figure 3 (b). Obviously the thick dendrites formed during directional solidification before water quenching. Under water quenching, a certain amount α phase might grow epitaxially from the primary α dendrites without the need of re-nucleation.

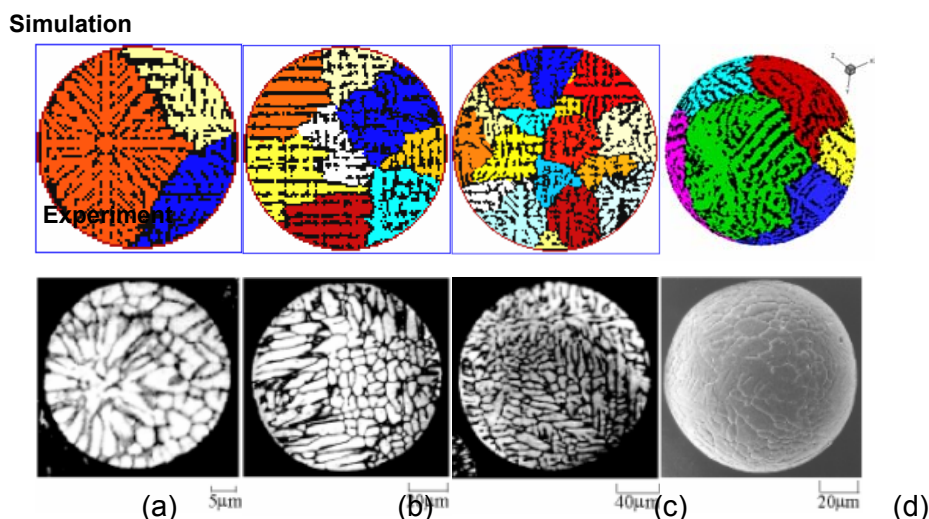


Figure 2: Simulated and experimental microstructures of atomized Al-10 mass%Cu droplets with various droplet sizes: (a) $40\mu\text{m}$, (b) $100\mu\text{m}$, (c) $200\mu\text{m}$ and (d) $100\mu\text{m}$. Here (a), (b) and (c) indicate the microstructures shown in 2-D cross section, and (d) 3-D view of a droplet.

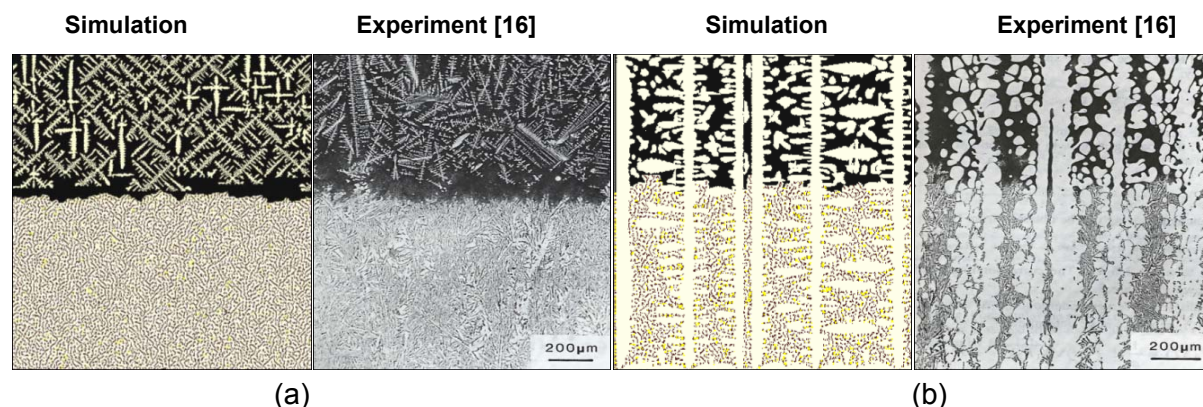


Figure 3: Simulated and experimental microstructures of Al-Si alloys directionally solidified at $G=15\text{ K/mm}$ and followed by water quenching: (a) Al-12.6mass% Si and (b) Al-8mass% Si.

4. Conclusion

A modified cellular automaton model has been proposed to model the evolution of microstructures in solidification of alloys. The present model includes nucleation, growth kinetics, the preferred growth orientation of crystals, and the solute redistribution in both liquid and solid phases during solidification. The effects of constitutional and curvature undercoolings are incorporated on the equilibrium interface temperature. Different numerical algorithms are employed for the growth of non-faceted and faceted crystals, and the mechanism of competitive and coupled eutectic growth is taken into consideration. The MCA model has been successfully applied to predict dendritic growth morphologies of Al-Cu alloys in two- and three-dimensional domains. The model can also be applied to model irregular eutectic growth patterns in eutectic and hypoeutectic Al-Si alloys.

Acknowledgments

The project (50371015) supported by NSFC and the project sponsored by SRF for ROCS, SEM.

References

- [1] W. J. Boettinger, S. R. Coriell, A. L. Greer, A. Karma, W. Kurz, M. Rappaz, and R. Trivedi, *Acta Mater.*, 48 43-70, 2000.
- [2] L. Nastac, *Acta Mater.*, 47, 4253-4262, 1999.
- [3] M. F. Zhu and C. P. Hong, *ISIJ Int.*, 41, 436-445, 2001.
- [4] M. F. Zhu, J. M. Kim and C. P. Hong, *ISIJ Int.*, 41, 992-998, 2001.
- [5] M. F. Zhu and C. P. Hong: *ISIJ Int.*, 42, 520-526, 2002.
- [6] C. P. Hong and M. F. Zhu, *Modeling of Casting, Welding and Advanced Solidification Processes X*, edited by D. M. Stefanescu, J. Warren, M. Jolly and M. Krane, TMS, Warrendale, PA, 63-74, 2003.
- [7] L. Beltran-Sanchez and D. M. Stefanescu, *Int. J. Cast Metals Res.*, 15, 251-256, 2002.
- [8] L. Beltran-Sanchez and D. M. Stefanescu, *Metall. and Mater. Trans.* 34A, 367-382, 2003.
- [9] M. F. Zhu and C. P. Hong, *Physical Review B*, 66, 155428, 2002.
- [10] M. F. Zhu, S. Nishido, and C. P. Hong, *Int. J. Cast Metals Res.*, 15, 273-278, 2002.
- [11] M. F. Zhu and C. P. Hong, *Modeling of Casting, Welding and Advanced Solidification Processes X*, edited by D. M. Stefanescu, J. Warren, M. Jolly and M. Krane, TMS, Warrendale, PA, 91-98, 2003.
- [12] M. F. Zhu and C. P. Hong, *Metall. Trans.* 35A, in press, 2004.
- [13] Ph. Thevoz: Sc. Dr. Thesis No. 765, Swiss Federal Inst. Tech., Lausanne, 1988.
- [14] B. Chalmers: *J. Aust. Inst. Met.*, 8, 255, 1963.
- [15] J. Lipton, M. E. Glicksman, and W. Kurz, *Metall. Trans.* 18A, 341-345, 1987.
- [16] R. Grugel and W. Kure, *Metall. Trans.* 18A, 1137-1142, 1987.
- [17] M. D. Hanna, S. Z. Lu, and A. Hellawell: *Metall. Trans.* 15A, 459-469, 1984.